Particle size segregation in granular flow in silos, with Rusal Aughinish

Technical Report from MACSI's 2012 Problem-Solving Workshop with Industry

Report MACSI/ESGI/0032

MACSI

Mathematics Applications Consortium for Science & Industry

Fondúireacht Eolaíochta Éireann
Science Foundation Ireland

Particle size segregation in granular flow in silos

Louise Clune and Martin Fennell
Rusal Aughinish, Limerick, Ireland

Davide Cellai[1], Vincent Cregan[1], Mark Curtis[2], Andrew Fowler[1],
John Hinch[3], Graeme Hocking[4], Mark McGuinness[5],
John Murnane[6], Stephen B.G. O'Brien[1], Nadia Smith[7]

[1]*MACSI, University of Limerick,*
[2] *Mathematical Institute, University of Oxford,*
[3] *University of Cambridge,*
[4] *Murdoch University,*
[5] *Victoria University of Wellington,*
[6] *University of Limerick,*
[7] *Universidad Complutense de Madrid.*

June 2012

Abstract

Segregation and layering of alumina in storage silos are investigated, with a view to predicting output quality versus time, given known variations in input quality on emplacement. A variety of experiments were conducted, existing relevant publications were reviewed, and the basis for an algorithm for predicting the effect of withdrawing from a central flowing region, in combination with variations in quality due to geometric, layering and segregation effects, is described in this report.

1   Executive Summary

Rusal Aughinish are required to accurately forecast quality of alumina shipments to customers. Historically, sometimes discrepancies exist between forecast and actual shipment quality. The problem presented to this Study Group was to:

1. Understand the segregation mechanisms of alumina

2. Predict particle size distribution of alumina exiting a silo

3. Predict other quality parameters of alumina exiting a silo

Further points to consider in the segregation analysis were:

1. does the alumina segregate as the silo is filling?

2. what is the impact of low silo levels?

3. how does the profile change during discharge?

4. what is the impact of air slides not operating?

5. what is the impact of sampling?

6. what is the impact of loading from more than one silo at a given time?

The Study Group conducted a number of experiments with materials of two different sizes, and found that there was segregation upon pouring evenly mixed material onto a pile, and extracting from a hole centered under the pile. In those experiments, finer material exits first. However, experiments conducted by Engblom (2012) indicate that for material similar to alumina, with a smaller median particle size than that used in the Study Group experiments, a different mechanism dominates segregation, resulting in more fine material further away from the place it is poured in. This radial segregation is observed by Engblom even when the silo has a central delivery tube with doors in it, to reduce entrainment of air by the fines. The result of this radial segregation, in combination with extraction from a centrally placed hole at the bottom of the silo, is that there is a marked increase in the percentage of fine material exiting when the silo is nearly empty, as illustrated in figure 1. This agrees with the experience of Rusal Aughinish.

The Study Group also considered a number of simple models for flow of material through a silo, and for mixing in a silo, culminating in a two-dimensional layer model that captures daily variations in input quality, and considers the various shapes of layers of different quality that might arise as a consequence, depending on input and output flowrates.

In broad terms, the layer model (illustrated briefly in figure 2) predicts that apart from a small initial amount of material in the flow funnel, extraction of material is largely from the top of the silo downwards, as material avalanches into the flow funnel at the centre of the silo. If there is material being placed in the top of the silo at the same time as it is extracted from the bottom, this material will short-circuit directly to the outflow, and will dominate the resulting quality. Otherwise, the top-down extraction process is
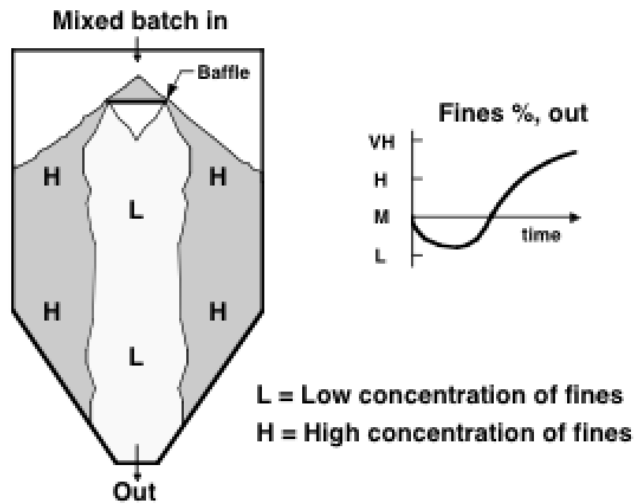
Figure 1: An illustration of results of an experiment with emplacement of material resulting in a higher concentration of fines near the walls of a silo, and the resulting output concentration of fines versus time, when extracting from a central hole with funnel flow (after Carson (1986), figure 4). The baffle is not relevant to the present report, but the distribution of fines is.
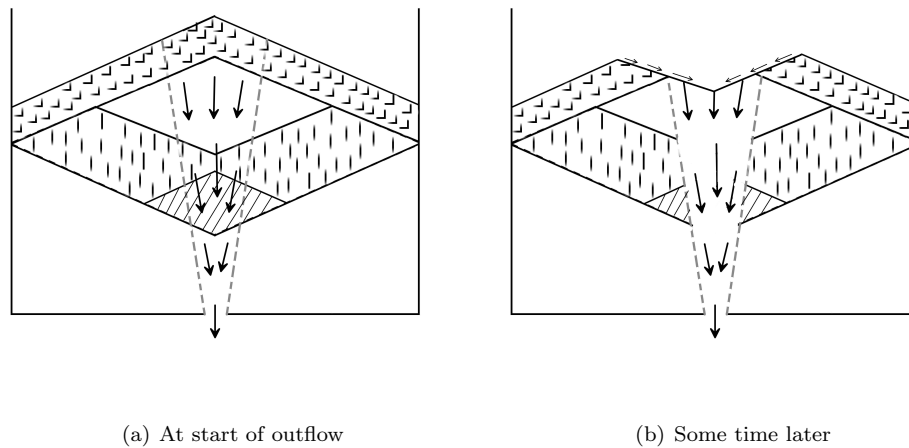

(a) At start of outflow

(b) Some time later

Figure 2: Sketches showing layers of alumina, shaded differently, of different quality placed on different days, to illustrate the kind of layering that can occur depending on flow history. The flow funnel is also illustrated with arrows and delineated with dashed lines. Flow into this funnel will occur initially from the top layer of alumina in the left-hand sketch, where an inverted cone at the angle of repose will develop from the centre, as illustrated some time later in the right-hand sketch. The right-hand sketch shows how material from two different layers is mixed as it avalanches into the flow funnel.

3

largely a FILO process (first in, last out), with mixing across any layers near the top of the current surface that were emplaced in such a way as to slope downwards towards the outer silo walls.

Also, any material that is near the silo walls and below a certain height, will not be accessed until fluidisation is used to assist flow of alumina when the silo is down to the last 40% of its capacity. This, in combination with radial segregation, will lead to a higher proportion of fines at this stage of emptying.

Other measures of quality, like the amount of iron present, may also be forecast (separately) using the layer model approach. Segregation will however also affect them, depending on what particle size they are associated with.

The work done in this Study Group forms a strong basis for developing a working algorithm for predicting the quality of alumina discharged from a silo, using layers of differing quality laid down on different days of net inflow, in combination with a simple radial segregation model, depending on parameters that should be determined by matching with data from the extensive Rusal Aughinish historical database.

2 Introduction

2.1 The Alumina Process

The Bayer process is used to make alumina (aluminium oxide, Al_2O_3) from the ore bauxite, which is then subsequently used in the production of aluminium. First, the bauxite (a silicate mineral which comprises alumina in the hydrated forms gibbsite ($Al_2O_3.3H_2O$ or just $Al(OH)_3$) and boehmite ($Al_2O_3.H_2O$ or just $AlO(OH)$), as well as other oxides such as those of iron and titanium, is dissolved in hot caustic soda solution NaOH:

$$Al(OH)_3 + NaOH \rightarrow Na^+ + Al(OH)_4^-;$$
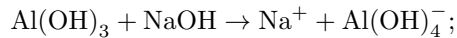
this process is called digestion. The other oxides do not dissolve and are filtered (clarification) and discarded as so-called red mud.

Next, the solution is cooled and seeded with alumina crystals, which act as nucleation sites and cause precipitation of the now super-saturated solution, so that the crystals grow in size until the liquid is poured off. The alumina crystals are then classified (those smaller than a certain size are recycled and used as seed crystals) and oven roasted to drive off the water leaving the alumina crystals (calcination).
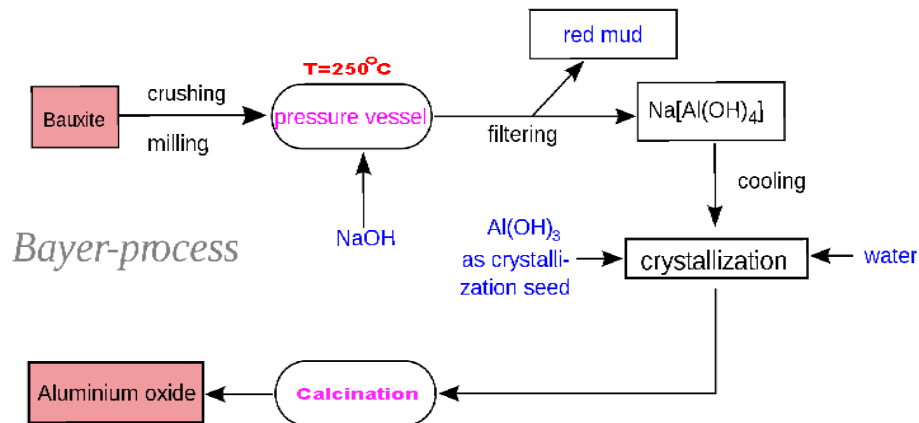

Figure 3: Overview of the Bayer process.

Following the production of the alumina crystals, they are stored in one of three silos. The floor is slightly sloping downwards toward the centre. The silos are fed from the top, from a conveyor belt that drops the alumina into vertical cylinders. These cylinders have doors in their walls, spiraling up, and opening when there is a higher pressure on the inside. These doors were installed to promote radial distribution of alumina. The crystals are withdrawn from the base through a series of about eight circular or elliptical holes. Air slides assist flow, both inside the silo on the floor, and below the silo in the exit channel. One silo is fed at a time. One or two (at most) of the silos silos may be emptied at the same time, with a conveyor belt going sequentially from one to the next, before carrying the alumina to a ship. Each silo can hold five days of production. The bulk density of the alumina powder is very close to 1 tonne/m^3.

Built into the inside of each silo floor is a series of air channels (*air slides*), on lines extending radially from the exit holes near the center to the walls of the silo. When the overpressure of alumina falls sufficiently, and the silo is nearly empty enough that alumina will no longer flow unassisted through the exit holes, these air channels are activated sequentially, radially outwards in one of six sectors, so as to encourage

Figure 4: A photograph of the top of one of the Rusal Aughinish silos, with the conveyor belts going to and from ships in the background.

alumina flow when the angle of repose is such that it might not otherwise flow to the exit holes. The gaps between air channels increase towards the silo walls, so that some alumina can never be mobilised.

It is not clear to what extent the air flow fluidises the overlying alumina, especially near silo walls where the overburden will be greater than the air pressure. It is clear that the air flow mobilizes the alumina, allowing extraction of more than without it.

2.2 The Problem

The problem facing the study group concerned the issue of quality control. Quality refers to a number of characteristics of the crystal feed, of which the one we were asked to focus on was particle size. The crystals typically have a near Gaussian grain size distribution, with a mean diameter near 100 μ, and a sub 45 μ fraction of typically 8%. Because of the variability of the production process, the quality of the crystal feed to the silos may sometimes be worse than this (higher fines means poorer quality).

Control of quality shipped then is possible, firstly by choosing which silo current production goes to depending on quality, then by mixing from one or two (at most) silos when loading a ship, with a view to meeting the desired criteria.

The input quality of the crystals entering a silo is monitored daily, and alumina is fed into one silo at a time, so that in principle the exit quality from each silo should be predictable. Indeed, Rusal Aughinish have a prediction algorithm, but it does not always work well, nor is there any record now of what principles it is based on.

Further information that arose from discussions with industry representatives indicates that when a silo is approaching empty is when the % of fines in the output is usually found to increase considerably.

3 Experimental analysis during Study Group

Aughinish wish to understand the mechanisms of particle segregation and mixing in the silo. Presently, the quantity of alumina in a silo is ascertained by taking dip measurements from the top of the silo, and

using these measurements to estimate the approximate volume, and thus tonnage of material in the silo. Product quality is measured before it enters the silo, and after it leaves the silos. However, the quality (or particle size fraction) of the output from a silo is not always predicted correctly. Hence, a fundamental understanding of both particle segregation and mixing in the silo is critical.

Simple experiments were performed during the Study Group, to investigate for ourselves the particle flow dynamics in the silos. Of particular interest were:

- the effects of particle segregation and mixing on size

- variations in the particle size fraction while the silo is emptying

The experimental setup consisted of a number of household items. A see through plastic bucket, with diameter 30cm and height 20cm, and a funnel, with a stem diameter of 1cm, were used to recreate the silo and the central feeding column, respectively. These dimensions modelled the silo to an approximate scale of 1:125. To model the gate at the base of the silo, a hole with diameter 3cm was drilled at the centre of the base of the bucket. Mixtures of couscous ('large' particles), sugar ('small' particles) and fine coffee powder ('fine' particles) were used in place of the alumina particles. The differences in the color of the particles were exploited to observe particle segregation and mixing.
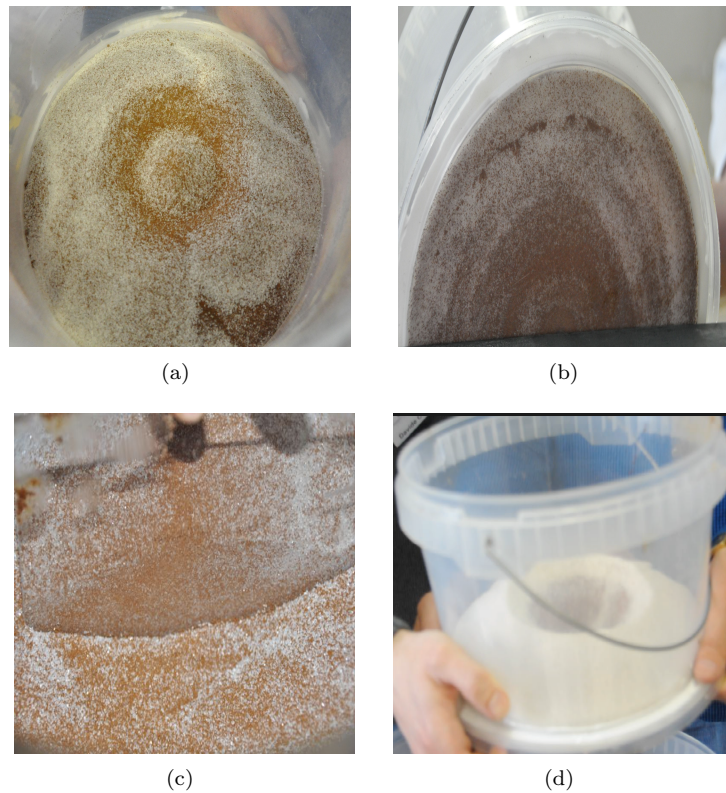

Figure 5: (a) Plan view of conical heap of sugar and coffee powder with coarser sugar overlying finer coffee on the surface of the heap (b) particle radial segregation viewed from beneath the bucket (c) cutaway sectional view within the bucket showing homogeneous mixture in heap interior and (d) formation of inverted cone during particle exiting at the bottom.

3.1   Particle segregation and mixing

Two separate experiments were carried out to investigate the behaviour and movement of the particles in the silos as they were filled and emptied. The first experiment was used to investigate segregation and mixing effects in the silo. Several possible particle mechanisms were considered including the separation of fine and coarse on the silo heap due to avalanches, and particle mixing and segregation due to material exiting at the base of the silo.

Initially, the hole at the base of the bucket was sealed, and a mixture of sugar and coffee was deposited into the bucket via the funnel. As expected, a conical heap of granular material was formed. Avalanches of material on the slopes of the heap were observed. As shown in Figure 5(a) the larger white sugar particles accumulated at the surface of the heap, while the smaller coffee particles moved downwards through the gaps between the sugar particles. This phenomenon has been extensively studied and modelled by Gray and Hutter (1997), Gray et al. (2003), Gray and Thornton (2005), and Gray et al. (2006). The smaller coffee particles are more likely to fall between the gaps that develop between the larger sugar particles. This results in an inverse grading of the particles whereby the larger particles rest on the smaller particles. In addition Figure 5(b), viewed from beneath a partially full bucket shows evidence of radial particle segregation. The larger particles have been transported to the base, and edge, of the bucket via the surface avalanches. To investigate the particle distribution within the heap a clear perspex tile was placed into the centre of the heap. One half of the heap was then removed to provide a cutaway sectional view. As shown in Figure 5(c) the mixture in the interior of the heap appears to be a homogeneous mixture of sugar and coffee.

Particle segregation and mixing during silo exiting was also examined. Sugar (large) was initially deposited in the bucket followed by a deposit of coffee (fine). These deposits created a cone shaped heap of material. The base gate was opened, and the material was allowed to flow out. An inverted cone-shaped hole rapidly formed at the centre of the heap as material from the preexisting cone exited through the hole. A little sugar came out first, rapidly followed by coffee from the top of the heap. Once the preexisting cone was removed, material fed into the inverted cone by a sequence of avalanches that flowed down the faces of the free surface at the angle of repose. As shown in Figure 5(d), these avalanches lead to the coarser material being removed first, and the faces of the inverted cone being covered in a fine layer of finer particles. We also observed mixing of the layers of coffee and sugar. Critically, this experiment validates the last in first out hypothesis whereby the material that makes up the top of the cone is the first to completely exit the silo.

3.2   Particle size fraction upon silo emptying

A second experiment was used to temporally quantify the fraction of fine particles exiting the silo. 'Large' couscous ≥ 1.18mm particles were sieved out and mixed with 'small' sugar particles ≤ 1.18mm to form a homogeneous mixture of 10% 'small' to 'large' by weight. The mixture was then dropped into the closed bucket via a centrally located funnel with a 1cm opening. Once all the material had been dropped in, the base gate was opened, and the mixture allowed to drop out. Samples of the exiting material were taken every 30s, and sampling continued until material ceased to flow. Each sample was weighed. The large particles were then sieved out and weighed and by subtraction the fraction of 'small particles was determined. Figure 6(a) shows the results from this part of the experiment.

After the particles stopped flowing, the base gate was replaced, and the heap was topped up with additional material consisting of a 20% small to large particle ratio by weight. The base gate was removed, and the sampling process was repeated as before. The small to large particle size results from this part of the experiment are shown in Figure 6(b).

Both experiments demonstrated that despite the initially low ratio of small to large particle sizes before exiting, the associated ratio during exiting started out quite high, then dropped, indicating that more fine particles were exiting early in the discharge. This is the opposite of the problem experienced by Rusal
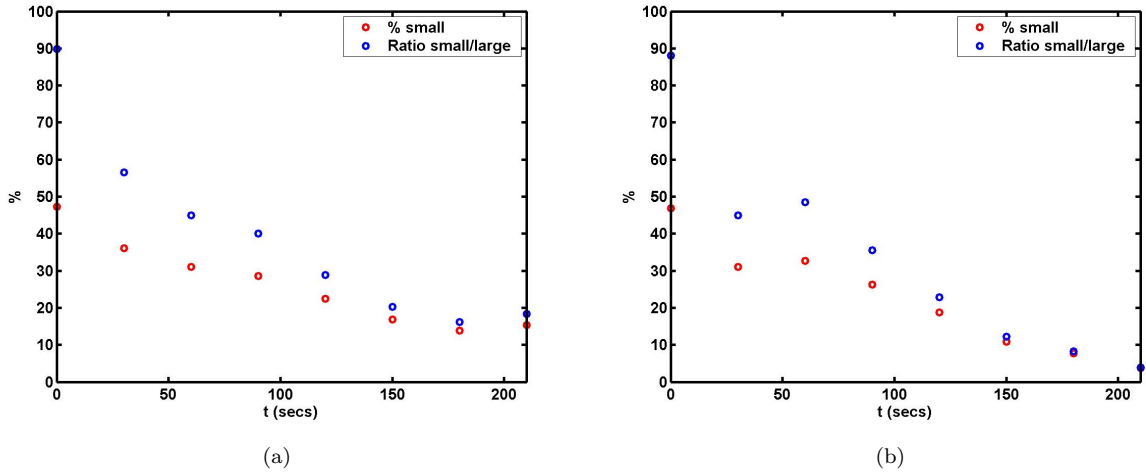
Figure 6: Experimental results for (a) initial material deposition with small to large particle ratio of 10% and (b) subsequent deposition with small to large particle ratio of 20%. Samples were taken every 30s as material exited the bucket. Sieves were used to separate the sampled material, and hence infer the raio of small to large particle size exiting the bucket.

Aughinish, but nevertheless illustrates segregation of fines in a silo.

4 One-Dimensional Models

The Study Group first considered some simple one-dimensional mathematical models for what could be happening inside the silo.

4.1 First in first out algorithm

The very simplest view of what happens in the silo, which would be appropriate if flow were of the type called mass flow, is the model that what comes into the silo first, goes out of it first (FIFO). The Study Group chose to consider this as the very simplest possible model, at one end of the spectrum of possible flows.

A continuous in-out flow model with no mixing leads to a nonlinear, 1d-advection equation for the quality ϕ,

$$\phi_t + w\phi_z = 0 \text{ with } \phi(h(t)) = \phi_{IN}(t), \quad w = -Q_{OUT}/A$$

This equation for $h(t)$ decouples so that $h(t)$ is known, given net inflow rate. The method of characteristics then gives $\frac{dz}{dt} = -w$, so that $dz = -w(t)dt$. To find the time lag, T for an incoming "particle" (at $t = t_0$) using

$$z(T) = h(t_0) - \int_{t=t_0}^{t_0+T} w(t)dt \Rightarrow z = 0 \text{ when } h(t_0) = \int_{t=t_0}^{t_0+T} w(t)dt$$

This can lead to rapid variations in output quality as the outflow rate changes.
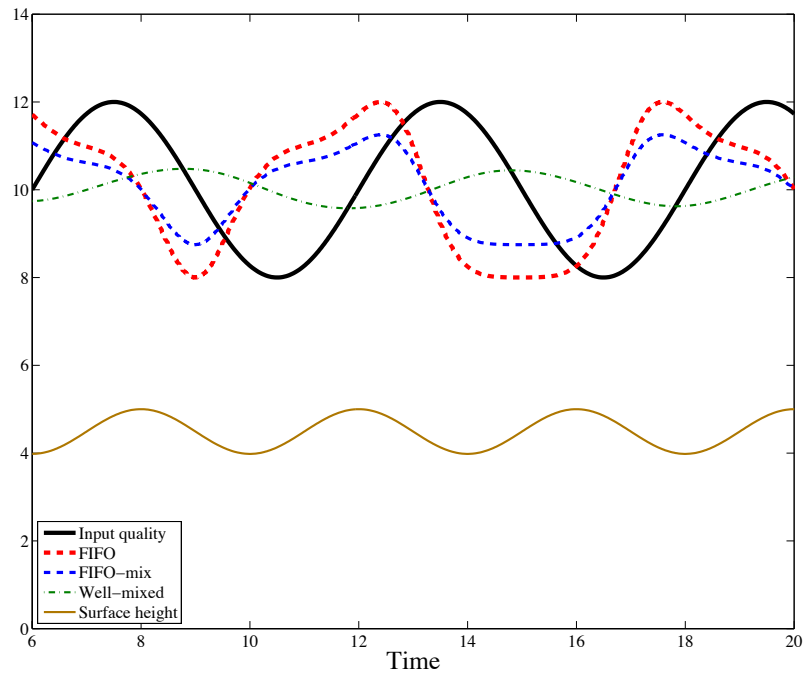
Figure 7: One-dimensional model results, for FIFO, partial mixing, and well-mixed cases. The inflow rate is held constant, with oscillating input quality. Discharge flowrate oscillates at a different frequency.

4.2 A well-mixed model

At the other end of a mixing spectrum of possibilities for flow is the assumption that material in the silo is well-mixed, before exiting. This may described mathematically by the lumped-parameter model,

- $h(t)$ = height of alumina column in silo (m)

- $V(t)$ = volume in silo (assumed = $h(t)A$ where A = area)

- $\phi(t)$ = quality of alumina (% <45μ) - high is undesirable

- $Q_{IN}(t)$ = volume flux of inflowing alumina (m^3/s)

- $Q_{OUT}(t)$ = outflux onto conveyer (m^3/s)

Then conservation of volume gives

$$\frac{dh}{dt} = \frac{Q_{IN}(t) - Q_{OUT}(t)}{A} \ ,$$

and taking the alumina to be well-mixed in the silo gives

$$h\frac{d\phi}{dt} = \frac{Q_{IN}}{A}\phi_{IN} - \left(\frac{Q_{OUT}}{A} + \frac{dh}{dt}\right)\phi \ .$$

4.3 FIFO with partial mixing

A simple model that combines the above two extremes is to assume there is some local mixing between adjacent batches of granular material. A batch, for example, might be one days load, of known quality, perhaps a different quality to the next days load. Using a moving average between adjacent batches gives behaviour that lies between FIFO and well-mixed. These three simple one-dimensional models are illustrated in Fig. (7). Rapid variations in discharged quality are apparent for the FIFO model, if variations in output flowrate are large enough.

5 Two-dimensional modelling

Two fundamental mechanisms are in play in alumina silos — segregation of fines from coarse due to a variety of mechanisms on emplacement and on discharge from the silo leading perhaps to more fines near the walls of a silo; and the fact that the percentage of fines also may vary from day to day, so that even if there were no segregation, there will be layering within the silo of regions with differing quality. First we will review some general principles and recent publications on segregation mechanisms and granular flow in a silo, then we will consider in some detail how to model the effect of layers formed in the silo by daily variations in quality.

6 Two-dimensional Flow in a Silo

Flow from a silo does not follow the simple first in first out description. When a granular material is poured on a surface, or on a container, it forms a conical surface whose angle of repose is that of the angle of limiting friction. In a silo, a volume with a two-dimensional conical surface is thus formed.

However, when emptying is done through a central basal hole, the basal material is not removed from the base, but rather flow is through a central funnel which takes the form of a central cone whose half-angle is around 15°, at least in the experiments of Gray and Hutter (1997), shown in figure 8. Outside this funnel, the material is at rest, but at the top surface, an inverted cone is formed at the angle of

repose. Material avalanches down this inverted cone and enters the funnel from above, sweeping across (and mixing) previously deposited layers of different quality as it proceeds downwards. Thus the filling and emptying processes cause effective mixing of the material deposited on different days, and these provide the basis for the mixing algorithm described here.

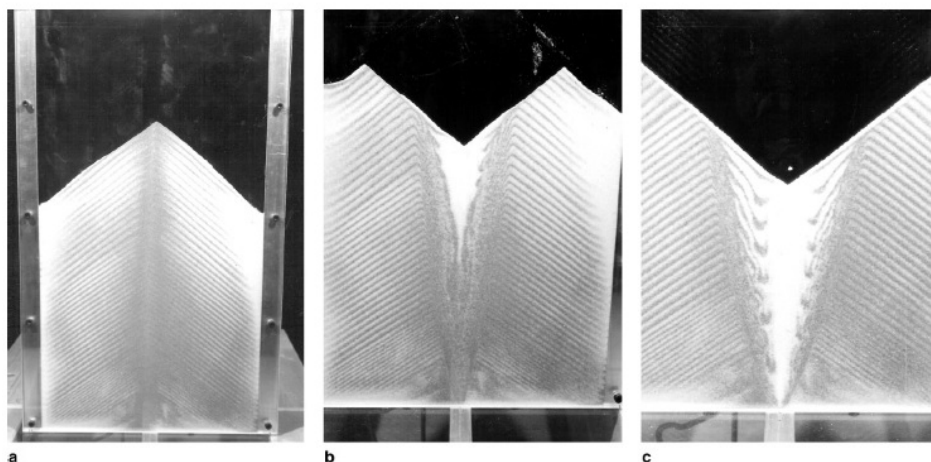## 6.1   Avalanching and surface segregation

Figure 8: Segregation during filling (a) and emptying (b) and (c). Reproduced from Gray and Hutter (1997), figure 3. The christmas tree appearance is due to darker fines separating from lighter coarse grains during filling, due to avalanching down the surface near the angle of repose. Also visible during emptying is the inverted conical flow region that extends from the exit hole to the surface. Flow into this conical region is by avalanching from the free surface, which can segregate fines to deeper than the free surface, progressively enriching that region in fines. Once in the conical region there is little segregation.

Continuous filling leads to a series of avalanches down the growing conical surface, and these cause fine scale segregation, in which small particles are able to pass below the larger particles, thus providing a fine scale striping, which can be seen in figure 8. The scale is not sufficient to warrant inclusion of this process in our model. More importantly, there is also a lateral segregation, which arises from the fact that the larger particles will flow further as they ride over the smaller ones underneath. This might have significance, but is also ignored in our discussion below. Furthermore, as discussed in section (6.3), other segregation mechanisms are likely to be in play in the Rusal Aughinish silos, since in fact observations suggest that the finer particles may in fact travel further due to air entrainment.

6.2   Withdrawal and funneling

The withdrawal process is illustrated in figure 8. Withdrawal is through a central cone which widens and which is fed by inverse avalanching from the developing inverted conical surface. Again the larger particles are able to override the smaller ones, and thus cause a segregated core of larger particles. This also can be important, although in our simple model this effect will also be ignored.

6.3 Segregation Literature Review

Segregation (and mixing) of granular material is a complicated subject with a large number of processes that may affect it in opposite ways. A number of publications by Gray and others explore the role of avalanching of material down slopes near the angle of repose on filling, while Ch. 13 in the book by Schulze (2008) illustrates nicely a wide variety of possible mechanisms for segregation when filling and when emptying silos of various design. The work of Kwade and Ziebell (2001) is relevant, being one of the few publications that contains case studies with measurements from experiments on silos, and they find that late production of more fines can be ameliorated.

In Carson et al. (1986) there is data presented on the segregation of tabular alumina, which may have a different size distribution to the Rusal Aughinish alumina. The PhD thesis by Engblom (2012) is also very useful, with a number of experiments on varying silo size and shapes, with varying granular materials. Engblom includes data taken from a silo that is in some respects a scale model of the Aughinish silos. These publications are relevant to our problem because they consider material with a distribution of grain sizes, and because they are firmly experiment based. Indeed, it is difficult enough to do mathematical modelling when the material consists of just two particle sizes, and a distribution of sizes is much more challenging.

The two flow types for discharge of granular material are mass flow, where all material in the silo is flowing, and funnel flow, where only material in a narrow conical region above the exit hole is flowing, leaving dead zones to the sides, and being fed into by material avalanching down the free surface near the angle of repose. These flows are illustrated in Fig. (9). The flow in the relatively wide silos at Rusal Aughinish is funnel flow, with a vertex angle that is possibly near 60° using the rough guide that the flow boundary is near the angle of repose away from vertical, as illustrated in Fig. (8). The vertex angle may however be closer to 30° judging by figure (8). The study group realised, and it is well known in granular flow, that funnel flow leads mainly to FILO (first in, last out) behaviour, after an initial period of FIFO (first in, first out) behaviour from the material initially in the funnel. This is discussed in more detail later.
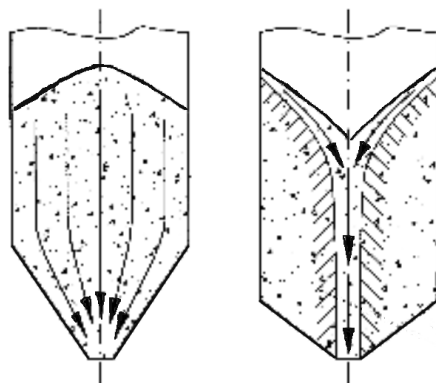
Figure 9: An illustration of mass flow (on the left) and funnel flow (on the right), after Kwade and Zeibell (2001). Which flow occurs depends on silo shape and dynamic slip angle for the granular material.

Kwade and Ziebell (2001) find that late production of more fines can be ameliorated by ensuring that outflow is mass flow, which gives good mixing of any radial segregation on exit from the silo.

The segregation mechanisms that are relevant to the Rusal Aughinish silos are rolling, sieving (these are often combined in the concept of kinetic sieving), air current, and embedding. These are illustrated in Figs. (10) and (11), and explained in the captions to those figures.

Inflow segregation by kinetic sieving would lead to the pine tree fine segregation pattern mentioned in the previous subsection, and studied by Gray and others, due to avalanching of inflow material down a
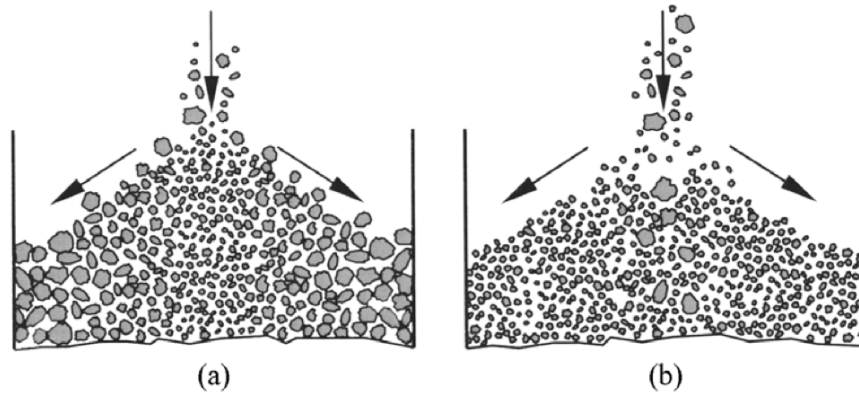
Figure 10: An illustration of (a) kinetic sieving, which includes sifting of fines through coarser crystals, and rolling of coarser crystals along the free surface; and (b) embedding, where aerated fines are penetrated by heavier coarse crystals. After Engblom (2012), originally from Schulz (2008).
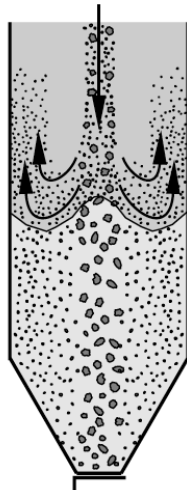
Figure 11: An illustration of the effect of air entrainment on entry to a silo, where fines below 50μ in diameter may flow further than coarse material due to their slower settling velocity in air. After Schulz (2008).

surface of repose. This gives a vertical segregation in the silo, but on a scale of millimeters, so fine that it seems irrelevant to the Aughinish problem. On outflow, however, the conical region of flow above the exit hole(s) is fed by avalanching down the free surface which is close to the angle of repose. That surface sweeps across the christmas tree segregation and might at first sight be expected to mix them. Kinetic sieving in this region, however, could also lead to fines dropping below the avalanche front, and since successive avalanches reach deeper and deeper, the sieving would be expected to continue, giving more and more fines just under the avalanching surface.

The work of Carson et al. (1986) suggests that the mean diameter of the alumina is too small at 100μ for there to be much kinetic sieving. Carson finds that for a mean diameter less that 200μ there is little kinetic sieving in practice. His figure 2 indicates that if there are just two particle sizes, and the mean diameter is 100μ, the ratio of diameters would have to be three or more to see more than 20% segregation coefficient, in comparison to 40% if mean diameter is 200μ. For a distribution of sizes, the effect will be even further reduced. So it is not clear that kinetic sieving is an important mechanism for Aughinish alumina.
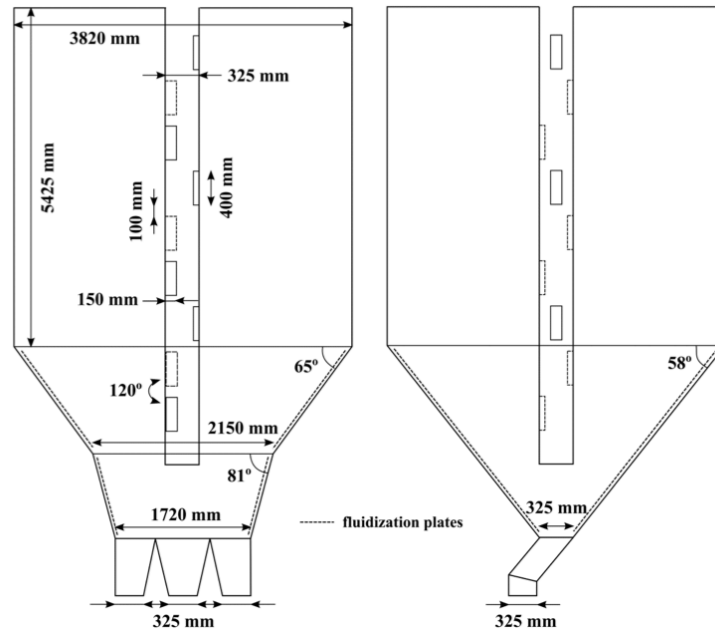
Figure 12: An illustration of the large silo used by Engblom (2012) in his experiments. Note the central tube with doors in it, to reduce air entrainment, a device also used in the Rusal Aughinish silos.

It is also unclear from the possible theoretical mechanisms whether there is a radial distribution of fines on entry to the silo, and whether such a distribution puts fines nearer the walls or nearer the centre of the silo. Air entrained by dropping alumina from a height can mobilise fines to travel further than coarser crystals. Avalanching tends to move coarse material further towards the walls, the opposite effect to air entrainment. A significant redesign of the Aughinish silos some years ago was to put in central tubes, with doors that open outwards when granular pressure is favorable. These tubes are intended to promote the radial distribution of alumina and to remove the tendency for dropped alumina to move more fines to the walls. Operator experience at Aughinish is that fines nevertheless remain more prevalent near the walls. The work of Engblom as described below strongly supports this experience.

Operator experience at Rusal Aughinish is that the percentage of fines increases when the last few

Figure 13: Percentage fines $<65\mu$ measured while filling, inside the 70m^3 silo used by Engblom (2012) in his experiments. The silo has been filled with material with a median size of 300μ. Filling is stopped at several levels, and measurements taken at the current surface at different radii. More fines are seen near the walls of the silo, up to twice the fines at the centre, despite the central delivery tube designed to reduce air entrainment.
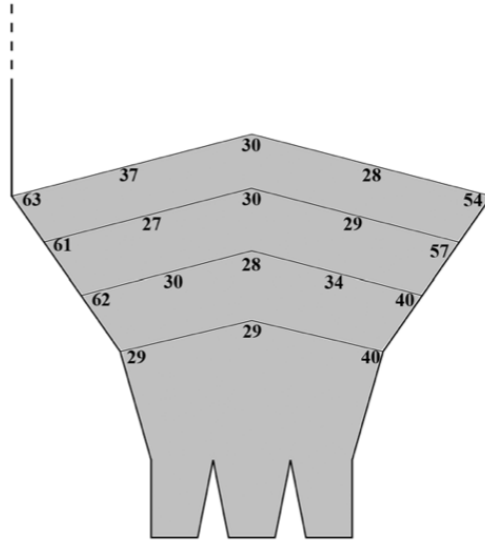
thousand tonnes of alumina in a silo are being unloaded. This is the same experience as the experimental results reported by Engblom (2012) for large and small silos, and by Kwade and Ziebell (2001). Engblom makes a careful experimental investigation (for cementitious materials generally larger than alumina, but with similar-sized fines) into whether the marked increase observed in percentage of fines at the end of emptying a silo is due to segregation of inflow, or to segregation during outflow from the silo. He concludes that the most important segregation occurs at inflow, not at outflow. That is, when the contents of a silo are carefully well-mixed, the troublesome increase in late fines is not seen in Engblom's experiments. However, funnel flow in the outflow process is also an important aspect, since mass flow is quite effective at re-mixing the radial segregation on outflow (and is the cure demonstrated by Kwade and Ziebell (2001)).

It is very interesting to note that the 70m^3 large silo used by Engblom has the same system as Aughinish, of a central delivery pipe with doors in it, to reduce air entrainment. Engblom's silo is illustrated in Fig. (12). Fluidisation plates on the sloping bottom blow air into the silo during discharge, but do not always fluidise the entire silo. Engblom measured percentage of fines in a granular material containing cement, sand and limestone and with a median grain size of 300μ, at various radial positions and at various surface heights, while filling with no discharge. Despite the presence of the central tube and doors, significantly more fines were found by Engblom at the walls of the silo during filling, as illustrated in Fig. (13). Discharging such a radial segregation with funnel flow means the high fines come out last, especially in the Rusal Aughinish silo geometry — this is discussed further later in this report.

When Engblom empties the silo with fines distributed radially as in Fig. (13), he has funnel flow, and there is a late increase in fines exiting the silo as illustrated in Fig. (14). Possibly the fluidisation also moves fines to the surface near the end of the flow, further segregating and delaying fines from exiting. Note that when Engblom empties a silo with mass flow (not funnel flow), emplaced radial variations in fines have almost no effect on fines exiting the silo, which emerge well-mixed at all times.

Also relevant to this problem but more confusing perhaps is the work done by Carson et al. (1986).
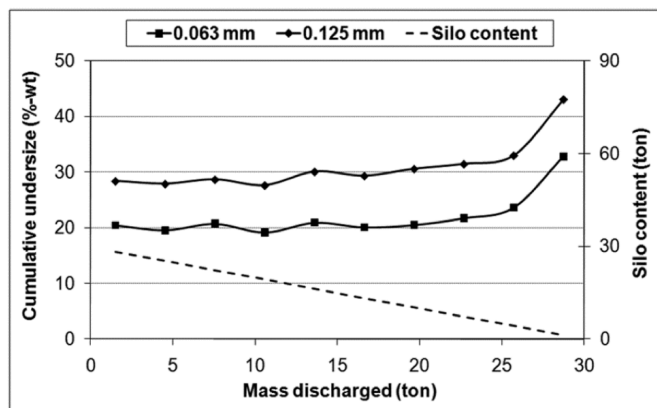
Figure 14: Cumulative percentage fines observed exiting the large silo used by Engblom (2012) and filled with material as illustrated in Fig. (13). Funnel flow occurs, and the radial distribution of fines leads to the late upturn in fines when the silo is nearly empty.

They observe that tabular alumina (which may have larger grains than here) generally has more fines in the place it falls, rather than at the walls. This is the opposite to the observations of Engblom of fines moving to silo walls, and to the experience of Aughinish operators.

7 Mixing in two dimensions

In this section, we focus on the effect of a varying quality of input to the silo, laid down in a series of layers over a period of several days.

In an ideal world, we might hope to build an internal flow field in the silo which allows for surface segregation due to avalanching on input, as well as funnelled withdrawal and segregation on output, together with variations in input quality. This is an ambitious goal, possibly unobtainable, and perhaps also unusable. Kinetic sieving may be only a minor player, compared with mixing and air entrainment, given Carson et al.'s results mentioned previously.

The algorithm we present here considers only the effects of mixing different qualities laid down on different days, due to variations in process quality entering the silo, and ignores segregation effects at this stage. The modelling is nevertheless still quite complicated conceptually, because the shape of the free surface can be complicated, and determines the lower boundary of material being deposited on it if there is net inflow. Hence layer shapes can be complicated to compute.

We begin by identifying four different states of the surface, as illustrated in figure 15; these states are labelled 1,2,3,4, and have crystal volumes V_1, V_2, V_3 and V_4, which are functions of wall height h, and in the case of states 3 and 4, the radius of the internal rim s. Explicit formulae follow from those for a cylinder of height h and radius r, $\pi r^2 h$, and for a cone of radius r and height h, $\frac{1}{3} r^2 h$. If we define the volume of a cylinder of radius r and height h surmounted by a conical roof with slope equal to the angle of friction θ to be $v(h, r)$, then

$$v = \pi r^2 (h + \tfrac{1}{3}\mu r),\tag{3.1}$$

where

$$\mu = \tan\theta\tag{3.2}$$

17
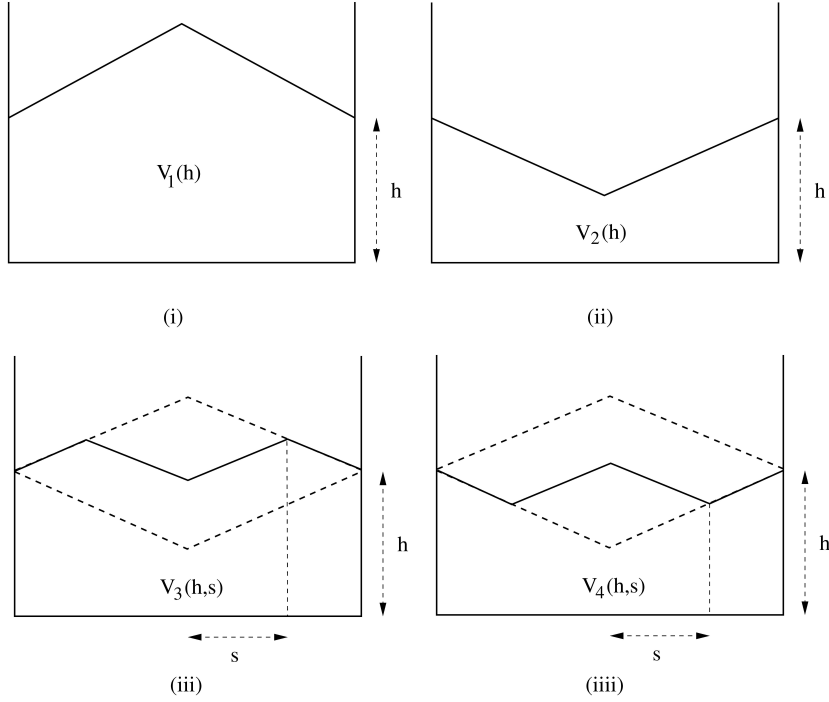
Figure 15: The four basic silo states.

is the static coefficient of friction. In terms of this, the crystal volumes in figure 15 are given by

$$
\begin{aligned}
V_1(h) &= v(h, r_S), \\
V_2(h) &= V_1(h) - 2v(0, r_S), \\
V_3(h, s) &= V_1(h) - 2v(0, s), \\
V_4(h, s) &= V_2(h) + 2v(0, s),
\end{aligned}
\tag{3.3}
$$

where r_S is the radius of the silo.

In the filling process, the distribution and avalanching of the crystals always causes a conical heap to form at the angle of friction. In emptying, a central dimple will form, yielding a depression whose downwards slope is limited by the angle of friction. We make the simplifying assumption that this limiting slope is reached instantaneously, so that the surface slope is always at the angle of friction, either upwards or downwards from the centre.

The emptying and filling processes allow transition between states, as follows: in emptying, we allow

$$
E_{12}, \ E_{13}, \ E_{22}, \ E_{32}, \ E_{33}, \ E_{42}, \ E_{44}^*,
\tag{3.4}
$$

where the notation E_{ab} means state a can be emptied to state b. The asterisked transition E_{44}^* is discussed further below. The corresponding transitions in filling are

$$
F_{11}, \ F_{21}, \ F_{24}, \ F_{31}, \ F_{33}^*, \ F_{41}, \ F_{44},
\tag{3.5}
$$

and the state F_{33}^* is also discussed below.

18

Our algorithm consists of identifying the state of the system after each filling or emptying event, and updating the quality variable $\phi(r, z)$, taken to be the fraction of fines $< 45\ \mu$. The algorithm thus produces a map for ϕ, and at the same time identifies exit quality during emptying events.

Given a state i, its current wall height h and internal rim radius s (if appropriate), and the distribution $\phi(r, z)$ of fines, we need to determine, for a volume change ΔV, the new state j, the new fines distribution $\phi'(r, z)$ and, if $\Delta V < 0$ (emptying), the mean exit quality $\bar{\phi}$. The full algorithm will thus contain fourteen variations, corresponding to the fourteen different transitions possible.

For filling with a quality (assumed constant) ϕ^*, we might wish to include a surface segregation, but this will be ignored. The vertical striping (Gray and Hutter 1997) is of too fine scale to be important. Longitudinal sorting, whereby the largest particles travel furthest, could be included if necessary, but is not included here.

As shown in figure 8 and discussed earlier, emptying is assumed to be through a central funnel of half-angle α, which in figure 8 is about $15°$ ($\tan \alpha \approx 0.26$). The simplest algorithm assumes that the width of the funnel is very small, so that the removed volume is that from the top of the pile. Roughly, this corresponds to the last in, first out scenario discussed earlier. The next complicating step would be to assume the instantaneous creation of a mature funnel, with its contained material being first removed, followed by material from the dimpled top surface. Again, we produce here only the algorithm corresponding to the simplest assumption.

7.1 Algorithm

We do not here include all fourteen state transitions, but simply illustrate the process for some state transitions. We take $\phi = 0$ where there are no crystals.

Emptying, E_{12}

To begin, we have state 1, wall depth h, crystal volume $V_1(h)$, and quality $\phi(r, z)$. If $\Delta V < -2v(0, r_S)$, then we are in transition E_{12}. The new value of h, h', is determined (uniquely) by

$$V_2(h') = V_1(h) + \Delta V, \tag{3.6}$$

the exit quality $\bar{\phi}$ is given by

$$-\bar{\phi}\Delta V = 2\pi \int_0^{r_S} \int_{h'-\mu(r_S-r)}^{h+\mu(r_S-r)} r\phi(r, z)\, dz\, dr, \tag{3.7}$$

and the new crystal fraction ϕ' is given by

$$\phi' = 0, \qquad z > h' - \mu(r_S - r),$$
$$\phi' = \phi \qquad z < h' - \mu(r_S - r). \tag{3.8}$$

In practice, we track $\phi(A, z)$, where $A = \pi r^2$, and then the integrals are simply approximated by a normalized sum over all the values on a discretized grid of A, z values.

Filling, F_{21}

This is simply the reverse of E_{12}. We are in state 2, with wall depth h, volume $V_2(h)$ and quality $\phi(r, z)$. For $\Delta V > 2v(0, r_S)$, the transition is to state 1, and the new value of h is determined uniquely by

$$V_1(h') = V_2(h) + \Delta V, \tag{3.9}$$

and the updated quality is

$$\phi' = 0, \qquad z > h' + \mu(r_S - r),$$
$$\phi' = \phi^*, \qquad h - \mu(r_S - r) < z < h' + \mu(r_S - r),$$
$$\phi' = \phi \qquad z < h - \mu(r_S - r), \tag{3.10}$$

where ϕ^* is the input quality.

Emptying, E_{13}

A slightly more complicated situation occurs in the transition to state 3. We begin in state 1 with wall depth h. If $-2v(0, r_S) < \Delta V < 0$, then the transition is to state 3. The wall depth remains the same, and the internal rim radius s is determined uniquely by

$$V_3(h, s) = V_1(h) + \Delta V, \tag{3.11}$$

and the corresponding rim height is

$$h_+ = h + \mu(r_S - s). \tag{3.12}$$

The exit quality is defined by

$$-\bar{\phi}\Delta V = 2\pi \int_0^s \int_{h_+ - \mu(s-r)}^{h_+ + \mu(s-r)} r\phi(r, z)\, dz\, dr, \tag{3.13}$$

and the updated quality is

$$\phi' = 0, \qquad z > h + \mu(r_S - r) \quad \text{and} \quad z > h_+ + \mu(r - s),$$
$$\phi' = \phi \qquad \text{otherwise.} \tag{3.14}$$

7.2 State closure: E_{44}^* and F_{33}^*

One can go on straightforwardly in this way. Complication occurs for emptying from state 4 and filling from state 3; we consider here the latter, and particularly the transition to a further state 3; the transition to state 1 is not problematic. The difficulty is illustrated in figure 16. For sufficiently small positive ΔV, a second internal rim is introduced, and thus in fact a new state in addition to the four in figure 15. It is easy to see that in fact subsequent emptying and filling can lead to an infinite number of further states, with an arbitrary number of internal rims. Consideration of such additional states leads to unnecessary complication, and we choose instead to introduce an approximate closure.

Starting from state 3 with wall height h, internal rim radius s and internal rim height h_+, we consider a sequence of fillings or emptyings of volume ΔV_i $i = 1, \ldots, n$, with input quality ϕ_i if $\Delta V_i > 0$, in which $0 < \Delta V_1 < 2v(0, s)$, and n is the first value for which either $\sum_i \Delta V_i < 0$ or $\sum_i \Delta V_i > 2v(0, s)$. In the former case, after n events, there is a genuine transition to a state 3, in the latter there is a transition to state 1. Up until event n, only the central shaded polygon in figure 16 is being altered, and we assume for $i < n$ that it is well mixed. Thus ϕ remains unaltered in the underlying pile during this sequence, while the quality ϕ_j of the shaded region after the j–th event and the corresponding exit quality $\bar{\phi}_j$ are defined by

$$\phi_j = \phi_{j-1}, \quad \bar{\phi}_j = \phi_{j-1}, \qquad \Delta V_j < 0,$$
$$\phi_j \sum_{i=1}^j \Delta V_i = \phi_j^* \Delta V_j + \phi_{j-1} \sum_{i=1}^{j-1} \Delta V_i \qquad \Delta V_j > 0, \tag{3.15}$$

where ϕ_j^* is the input quality for $\Delta V_j > 0$ (there is of course no exit quality during filling events).
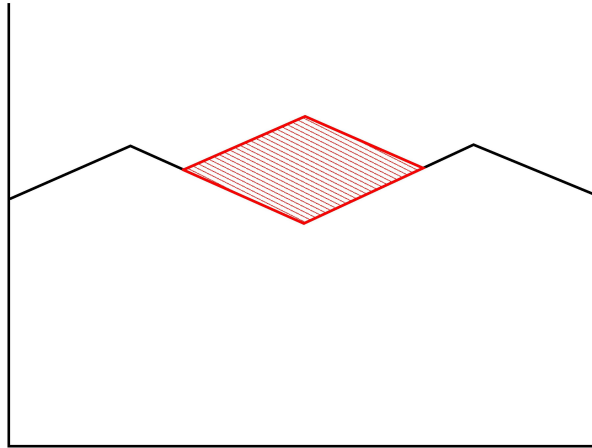
Figure 16: Filling state 3.

7.3 Final emptying

The algorithm above has to be adjusted when the silo becomes sufficiently empty, as shown in figure 17. This is when the residual crystal pile at the limiting angle of friction reaches the base of the silo in the centre. At this point, the air blowers are switched on below the silo, fluidising the stagnant pile and allowing it all to escape. Most simply, we assume that when this is done, all the remaining crystals are removed.
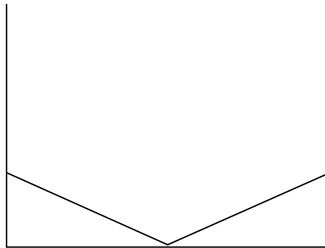
Figure 17: Final emptying

7.4 Strategy for poor quality input

Although the output quality is variable, it is generally rather constant, in the range of 8 or 9% fines. This suggests that when shipment quality fails, it is because of the radial segregation considered in previous sections. If a batch of poor quality, containing a high percentage of fines, is fed to a silo, as shown in figure 18, then successive emptyings will cause mixing of the output, and so long as emptying is done gradually (by using other good quality silos), it should be feasible to manage the occasional bad output. Hence one suggestion is to make sure bad quality alumina is only fed into reasonably full silos; this will prevent the situation where poor quality invades the dead space of figure 17.

The present policy of putting poorer quality material into one silo, and better quality material into
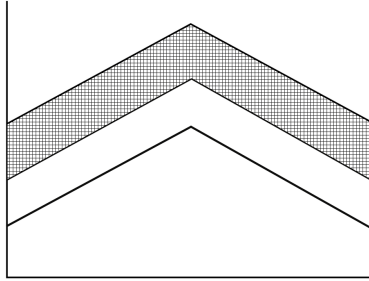
Figure 18: Managing poor quality input

Day	Mass in	Mass out	ϕ^a_{in}	ϕ^b_{in}	ϕ^a_{out}	ϕ^b_{out}
1	V_1		8.4	9.8		
2	V_2		8.8	9.7		
3	V_3	V'_1	8.8	8.2	9.5	8.5
4	V_4		7.6	8.6		
5	V_5		7.8	8.3		
6	V_6		7.8	7.9		
7	V_7	V'_2	7.8	7.6	7.8	8.2

Table 1: Data showing the mass entering a silo each day, and its quality on entry, and the mass taken from that silo and its quality on exit. Two measures of quality are used, ϕ^a and ϕ^a. They are Malvern and Rotap methods for measuring the percentage of alumina that is less than 45 microns in diameter.

another, is very sensible and possibly optimal, as it allows better control of subsequent mixing straight onto the exit conveyor belt.

8 An Instantiation of Models

Data was provided to the Study Group during a time when only one silo was loaded and used, as a simple example. This data is presented in Table (1), and shows the amount of material and its quality entering the silo each day ("Mass in"), and the amount of material and its quality measured on the way to a ship ("Mass out").

This data is used here to compare some of the 1D and 2D models that have been discussed previously.

8.1 FIFO model

The discharge on day 3 is assumed to come from day 1 input, so would have quality (a) 8.4 or (b) 9.8. This does not agree very well with the measured values.

The discharge on day 7 is assumed to come from days 2, 3 and part of 4, giving an average quality of (a) 8.7 or (b) 9.5. These are higher than the measured values of (a) 7.8 and (b) 8.2.

8.2　2D mixing algorithm

Not enough historical data is used here to be sure of the shapes of surfaces/regions of different quality, but a simplified approach is taken. We assume an angle of repose of 30° and that the flow funnel has opening angle 60°. We also assume that the silo is empty when day one material (V_1) is deposited, so that the shape of the day one region is as sketched in Fig. (19(a)).

Then day 2 is added, V_2, to give the shape sketched in Fig. (19(b)). Day 3 is then added with V_3, as sketched in Fig. (19(c)).

(a) Day 1 filled region　　　　(b) Days 1 & 2 filled regions　　　　(c) Days 1, 2 & 3 filled regions

Figure 19: Schematics of filling region shapes

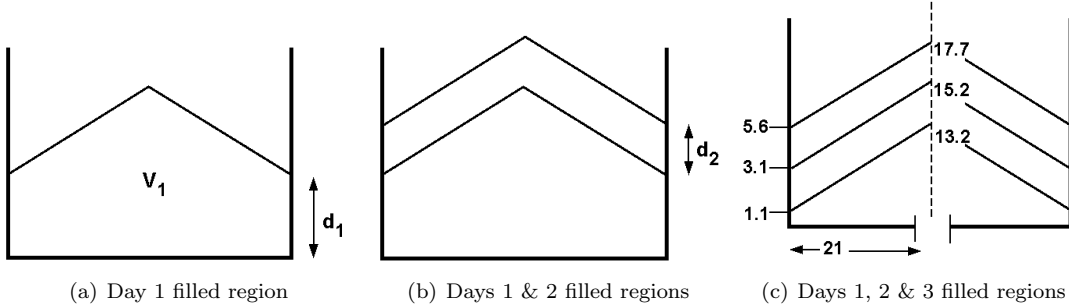Then on day three alumina is extracted, leading to the shaded region as sketched in Fig. (20(a)) being removed from the silo. It is a fairly simple matter to calculate (e.g. by slicing with cylinders and breaking the integration up piecewise) the volumes taken of days one, two and three. Using these to weight the qualities from those days gives a predicted overall quality of (a) 8.6 and (b) 9.2 for the shipment. These values are closer to the measured values 9.5 and 8.5, but still don't match, possibly due to the assumption that we have started with an empty silo. In fact, it is clear that the value 9.5 cannot come from any averaging of the previous three days' values which all lie below 8.9.

The modelling was continued through to day seven, assuming that fluidisation occurred on day three, reducing the shape of the alumina remaining in the silo, before adding days four through seven in layers as before, and removing the region sketched in Fig. (20(b)) of volume V_2'. Calculating volumes for the previous events, days 1–3 mixed up in the fluidised region, days 4-7 in layers on top, gives volumes 54, 509, 1147, 2399 and 3391 respectively, and an overall quality of (a) 7.8 and (b) 7.9. The (a) value matches exactly with the measured value, and the (b) value is close to the measured value of 8.2.

This exercise in matching the mixing layer model to data has been very useful, first to gain some confidence that the model matches quite well with data, and to illustrate the simple geometry leading to not-so simple mixtures of previous days' qualities. No allowance has been made in this work for the possibility of radial segregation of fines, given the uncertainties surrounding this mechanism.

9　Discrete Simulations

A different approach, that still captures the mixing of layers and the order in which layers are accessed, is to consider the movement of alumina in packets, with rules to mimic the action of gravity and the angle of repose. To illustrate with a two-dimensional case, Figs. (21) and (22) show results of a numerical simulation, symmetric about the left-hand side, with feed of new packets at top left (that is, the middle of the full shape), and with removal at bottom left (the middle of the full shape). The rule used for moving is that a packet slips down to a lower neighbour if the upper one is higher by more than one unit. A

(a) Day three extraction

(b) Day seven extraction, left half of the region only
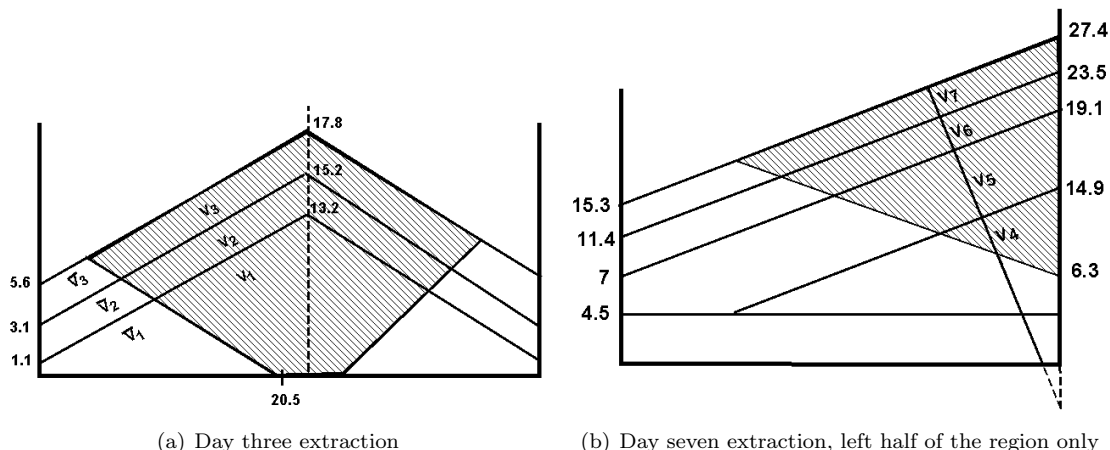
Figure 20: Schematics of extracted region shapes.

sequence of feeding and removing is illustrated, and the stream of packets output is also shown, numbered according to the layer they came from. That is, the numbering shows the quality of the current output, and averaging is evident in the mixing of the orders of the layers. The numbering could be taken to be the day number. Note the mixing that occurs here, in the output stream.

10   Segregation lattice model

A simple lattice model was considered and partially implemented, to describe segregation. Here is a brief description of this model.

Two types of particles of different size are allowed for, and size is represented on a lattice with a maximum allowed number of nearest neighbours c. For example:

- Particle A can have at most $c_A = 3$ neighbours.

- Particle B can have at most $c_B = 6$ neighbours.

(Particle A is larger than particle B)
  Specifications:

- Parallelepipedal rectangular lattice.

- Particles can only move down or horizontally.

- Horizontal movements tend to reproduce the correct angle of repose ($\sim 30°$).

11   Data analysis

The Study Group had time for only a very brief look at more extensive data from the Aughinish operation. A simplified view of some of that data, which ignores the choices made of which silo to put the alumina in, and which silo(s) to take it out of, is presented in Fig. (11). Such data will be essential for validating any detailed simulator that might arise out of this work. Note particularly the large time lag apparent in the quality of the output.

charge 1 of 120

```
1
11
111
1111
11111
111111
1111111
11111111
111111111
1111111111
11111111111
111111111111
1111111111111
11111111111111
111111111111111
```

(a) Day one filling

charge 2 of 120

```
2
22
222
2222
22222
222222
1222222
11222222
111222222
1111222222
11111222222
111111222222
1111222222
11111112222222
111111112222222
1111111112222222
11111111112222222
111111111112222222
1111111111112222222
11111111111112222222
111111111111112222222
1111111111111112222222
```

(b) Day two filling

charge 3 of 120

```
3
33
333
3333
33333
233333
2233333
22233333
222233333
2222233333
22222233333
122222233333
1122222233333
11122222233333
111122222233333
1111122222233333
11111122222233333
111111122222233333
1111111122222233333
11111111122222233333
111111111122222233333
1111111111122222233333
11111111111122222233333
111111111111122222233333
1111111111111112222222233333
```

(c) Day three filling

discharge of 180

```
3
333
33333
2233333
2222233333
22222233333
11222222233333
1111222222233333
111111222222233333
11111111222222233333
1111111111222222233333
311111111111222222233333
31111111111111222222233333
```

(d) Day three extraction (discharge 1)

charge of 120

```
4
44
444
4444
44444
444444
4444444
44444444
444444444    3
4444444444 333
44444444442233333
4444444442222233333
44444444422222233333
44444441122222233333
444444411122222233333
4444441111122222233333
444441111111222222233333
44441111111112222222233333
4311111111111122222222233333
31111111111111122222222233333
```

(e) Day four filling

charge of 120

```
5
55
555
5555
55555
555555
5555555
45555555
445555555
4445555555
44445555555
444445555555
4444445555555
44444445555555
444444445555555
44444444455555555
4444444445555355553555
444444444445333555
444444444444433333555
444444444442233333555
444444444422222233333555
44444444422222233333555
4444444411222222233333555
44444441111222222233333555
444441111111222222233333555
4444111111111222222233333555
44411111111111222222223333355
4311111111111122222222333355
3111111111111112222222333333555
```

(f) Day five filling

charge of 120

```
6
66
666
6666
56666
556666
5556666
55556666
555556666
5555556666
55555556666
555555556666
4555555556666
44555555556666
444555555556666
4444555555556666
44444555555566666
444444555555566666
4444444555555566666
444444444555555556666
4444444444555555536666
444444444445333556666
44444444444533335556666
4444444444433333555666
44444444442233333556666
4444444442222233333556666
44444444422222233333556666
444444411222222233333556666
4444441111222222233333556666
444441111122222223333356666
4444111111112222222233333556666
4441111111111222222233333355666
431111111111112222222233333556
31111111111111122222222333333556
```

(g) Day six filling

discharge of 180

```
6
6666
566666
5556666
5555566666
55555556666
445555535556666
4444453335556666
444444333335556666
4444442233335556666
444444422222333335556666
64444442222223333355666
644444441122222223333355666
54444441111222222233333556666
5444411111112222222233333556666
4441111111111222222233333556666
43111111111111222222233333355666
41111111111111122222223333333556
```

(h) Day six extraction (discharge 2)

discharge of 180

```
6
666
56666
5556666
335556666
33335556666
2333335556666
222233335556666
22222233333556666
1222222233333556666
111222222233333556666
11111222222233333556666
1111111222222233333556666
111111111222222233333355666
11111111111222222233333556
```

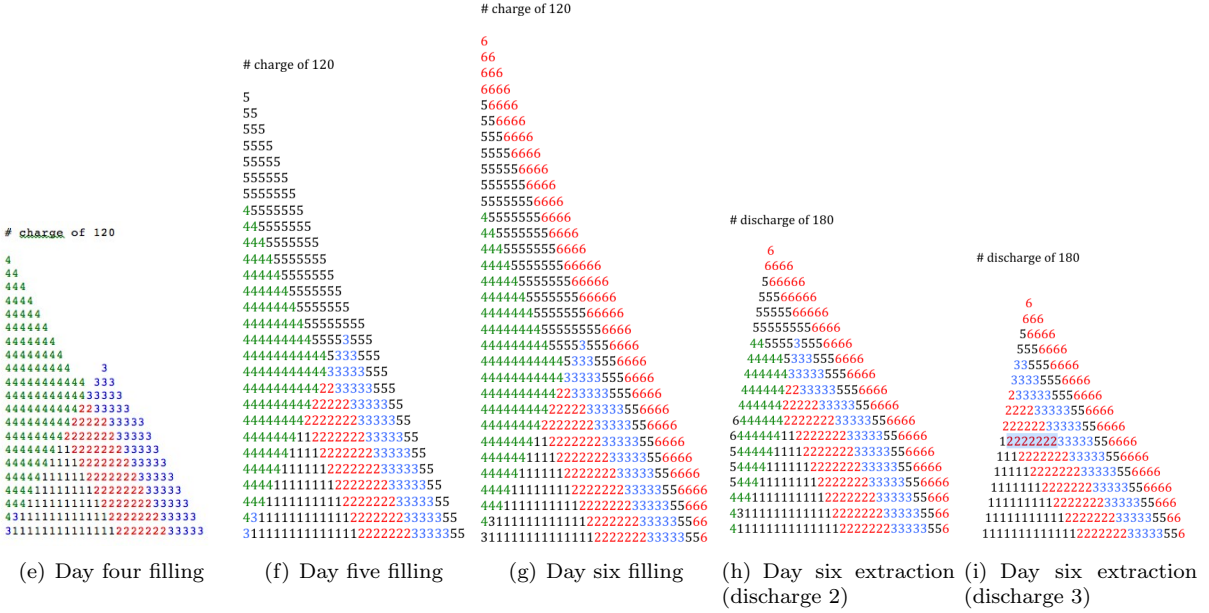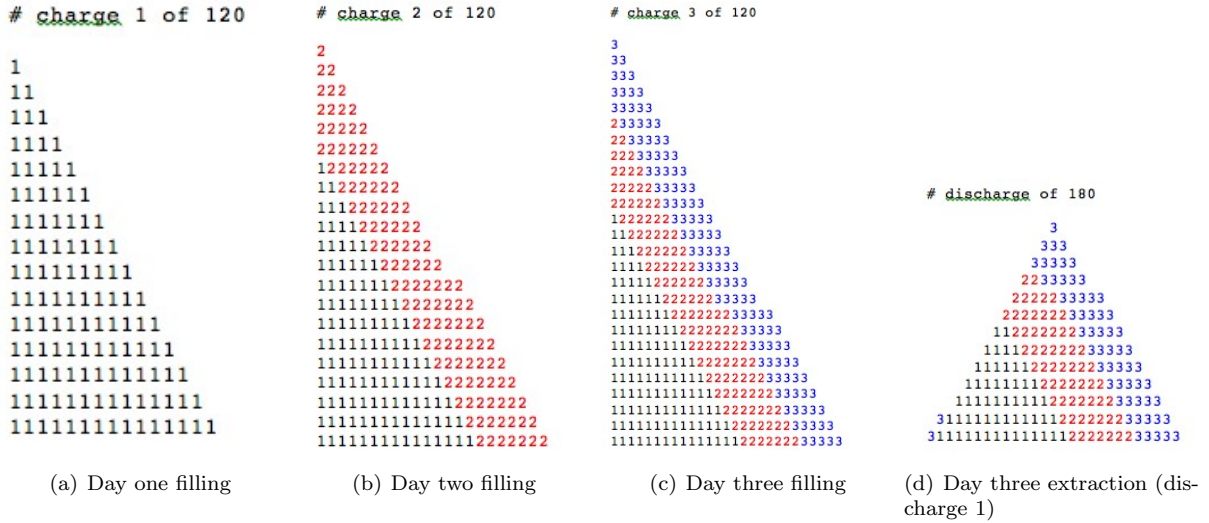(i) Day six extraction (discharge 3)

Figure 21: Sketch of discrete simulation sequence, three days of filling followed by one extraction, then three more days of filling, then two extractions until no more will flow. Note that only the right half of the symmetric figure is shown.

discharge 1

```
1 1 1 1 1 1 1 1 1 1 1 1 1 1 2 2 2 2 2 2 3 3 3 3 3
3 3 3 3 3 3 3 3 3 2 3 3 2 3 3 3 2 2 3 3 2 2 3 3 3 2
2 2 3 3 2 2 2 3 3 3 1 2 2 2 3 3 1 2 2 2 3 3 3 1 1 2
2 2 3 3 1 1 2 2 2 3 3 3 1 1 1 2 2 2 3 3 1 1 1 2 2 2
3 3 3 1 1 1 1 2 2 2 3 3 1 1 1 1 2 2 2 3 3 3 1 1 1 1
1 2 2 2 3 3 1 1 1 1 1 2 2 2 3 3 3 1 1 1 1 1 1 2 2 2
3 3 1 1 1 1 1 1 2 2 2 3 3 3 1 1 1 1 1 1 1 2 2 2
```

discharge 2

```
3 4 4 4 4 4 4 4 4 4 4 4 4 4 4 4 4 4 4 4 4 5 5 5 5 5
5 5 6 6 6 6 6 6 6 6 6 6 5 6 6 5 6 6 5 5 6 6 5 5 6 6
5 5 5 6 6 5 5 5 6 6 5 5 5 5 6 6 4 5 5 5 6 6 4 5 5 5
5 6 6 4 4 5 5 5 6 6 4 4 5 5 5 5 6 6 4 4 4 5 5 5 6 6
4 4 4 5 5 5 5 6 6 4 4 4 4 5 5 5 6 6 4 4 4 4 5 5 5 5
6 6 4 4 4 4 4 5 5 5 6 6 4 4 4 4 4 5 5 5 5 6 6 4 4 4
4 4 4 5 5 5 6 6 4 4 4 4 4 4 4 5 5 5 5 6 6 4 4 4 4
```

discharge 3

```
4 4 4 5 5 5 6 6 4 4 4 4 4 4 4 4 5 5 5 5 6 6 4 4 4 4 4
4 4 4 5 5 5 6 6 4 4 4 4 4 4 4 4 5 5 5 5 6 6 4 4 4 4
4 4 4 4 4 5 5 5 6 6 6 4 4 4 4 4 4 4 4 4 5 5 5 6 6
3 4 4 4 4 4 4 4 4 4 5 5 5 6 6 6
```

Figure 22: The discharges noted in Fig. (21) are detailed here, showing the order in which the layers (qualities) come out. Note there is FIFO then mixing evident.
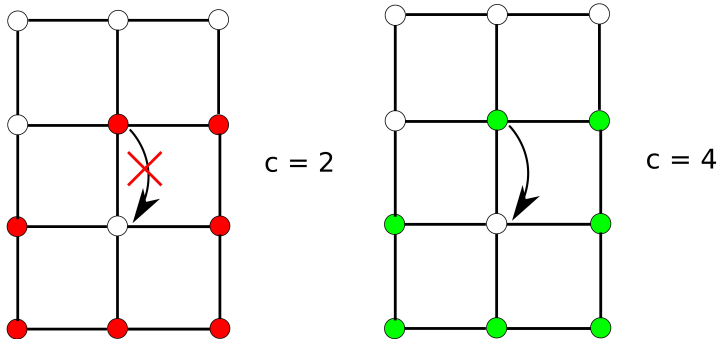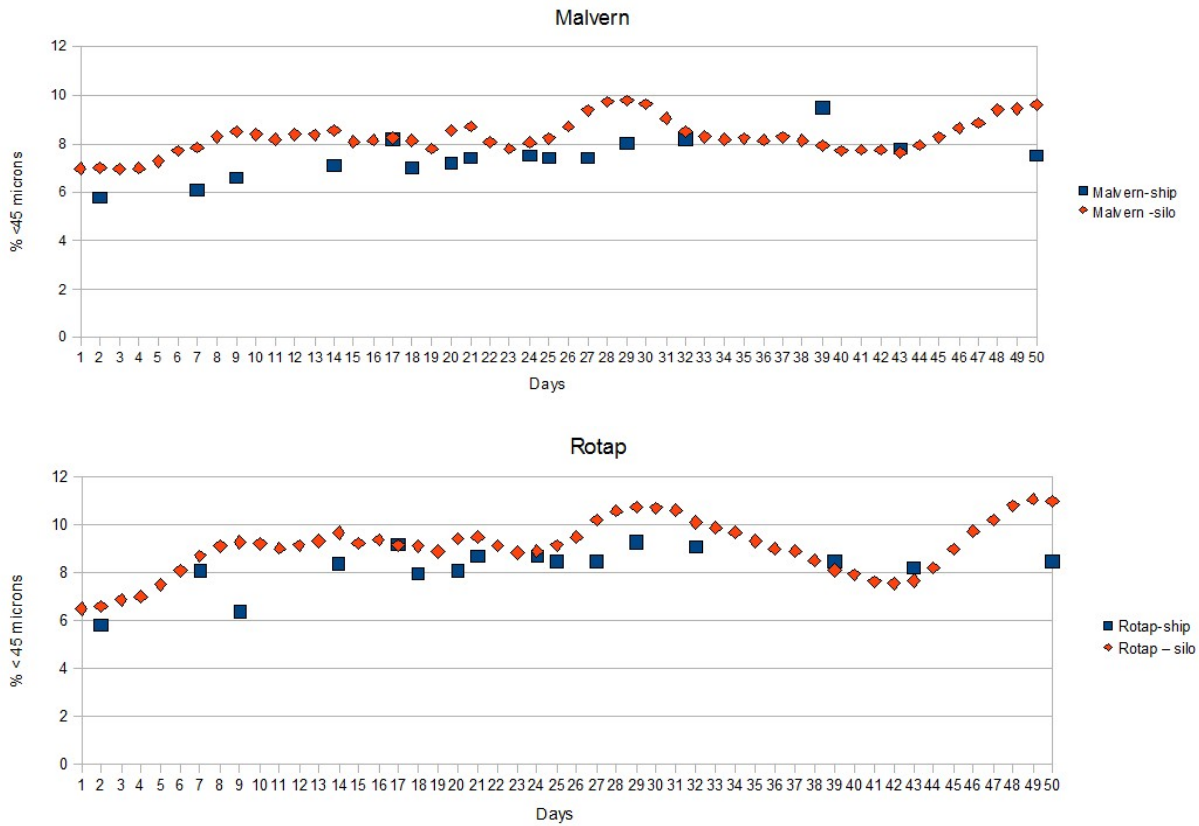

Figure 23: Examples in 2D

Figure 24: Data on percentage of fines in the input to silos, and in the output to ships, from the Malvern and the Rotap measurement processes.

12   Silo Geometry

It is useful to note some simple geometric consequences of silo shape, for amounts of alumina in silos and with segregation in mind. A silo has a capacity of about five days of production.

One day's production put into an empty silo will barely reach the walls, but will be piled about a third of the height of the silo at the centre. Each day after that, the height of the pile will go up the wall by about a sixth of the height of the silo.

The size of the flow funnel, if it has an opening angle of $60°$, is approximately 25% of capacity if the silo is full. Likely the flow funnel is much smaller that this, since the opening angle may be more like $30°$, which would reduce this volume to less than 8%. This suggests the volume of the flow funnel may be negligible (less than 3% capacity) for a silo that is less than half-full.

If there is radial segregation, perhaps increasing fines in the outer one-third of the silo radius, it is useful to consider how much of this remains at the point that fluidization is necessary to have outflow of alumina. The total volume remaining at the point that granular flow stops without air assistance is about 40% capacity, a pile with zero height at the centre and reaching just over half way up the outer walls. The outer one-third of this, possibly relatively high in fines, is about 30% capacity.

13   Conclusions

A number of modelling approaches have been taken to the question of what happens to the percentage of alumina less than 45 microns in size, between being placed in one of three silos, and being transported to a ship on a conveyor belt. The mechanisms of segregation and mixing have been thoroughly explored, through experiments, reference to published material, and a variety of mathematical models of increasing complexity and faithfulness.

Despite the central diameter tube placed in silos to reduce air entrainment, it is likely that the ongoing issues noted with an increase in percentage of fines when alumina levels get low in a silo are associated with two factors:

1. radial segregation on emplacement, due to air entrainment mobilizing fines and moving them closer to silo walls than larger crystals, and

2. removal of alumina from holes near the centre of the silo by funnel flow, delaying transport of fines near walls until the silo is nearly empty and fluidization is necessary to further remove alumina. This is not segregation as such, so much as the order in which material is removed.

If either of these factors is missing, it is expected that variations in measured quality exiting a silo would be relatively small.

The degree of segregation in the Rusal Aughinish silos could be quantified by either taking measurements in situ (which is probably too disruptive), or by two-dimensional modelling of funnel flow and layering, in combination with a simple segregation model that is then fitted to historical data to quantify the unknown parameters in the segregation model. Historical data will be most useful if detailed sample results are available for each ship, rather than an average of all sampling results for a ship.

The two-dimensional funnel flow and sweep model that is developed theoretically in this report serves as an excellent basis for producing a working simulator, that takes as input the historical flowrates and qualities entering each silo, and predicts the output quality from each silo or from a combination of silos. Note that since this model is a mixing model that presently does not account for segregation, it is equally applicable to other measures of quality of alumina, such as the percentage of iron present, or other contaminants.

Furthermore, segregation potentially affects these other measures of quality, if for example iron occurs as separate particles with some size distribution in themselves, or if it is found more or less frequently in or on smaller or larger alumina crystals.

Acknowlegements

References

Carson, J.W., T.A. Royal and D.J. Goodwill, (1986) Understanding and Eliminating Particle Segregation Problems, Bulk Solids Handling, 6(1), 139–144.

Engblom, N. (2012) "Segregation of powder mixtures in silos with particular reference to dry mineral-based construction materials", PhD thesis, Thermal and Flow Engineering Laboratory, Department of Chemical Engineering, Division for Natural Sciences and Technology, bo Akademi University.

Gray, J. M. N. T. and K. Hutter (1997) Pattern formation in granular avalanches. Cont. Mech. Thermodyn. **9**, 341–345.

Gray, J. M. N. T., Shearer, M. & Thornton, A. R. (2006) Time-dependent solutions for particle-size segregation in shallow granular avalanches. Proc. R. Soc. Lond. A 462, 947–972.

Gray, J. M. N. T., Tai, Y. C. & Noelle, S. (2003) Shock waves, dead-zones and particle-free regions in rapid granular free-surface flows. J. Fluid Mech. 491, 161–181.

Gray, J. M. N. T. & Thornton, A. R. (2005) A theory for particle size segregation in shallow granular free-surface flows. Proc. R. Soc. Lond. A 461, 1447–1473.

Kwade, A., and Ziebell, O. (2001) "Reducing the segregation of multi-phase plaster by selective alteration of the silo geometry", ZKG International, 54(12), 680–688.

Schulze, D. (2008) Ch 13 on *Segregation* in "Powders and Bulk Solids — Behaviour, Characterization, Storage and Flow", Springer. DOI:10.1007/978-3-540-73768_1_13